北見工業大学研究報告
第18巻 第1号 (昭和61年)

Memoirs of the Kitami Institute of Technology
Vol. 18 No. 1

Transient Characterization of Carbon Monoxide, Carbon Dioxide and Oxygen Adsorbed on MgO and $MgCO_3$*

by Yasuyuki KONISHI**, Toshio KATAGIRI***, Shuichi YASUI****, Yoshinori NAKANISHI*****, Tohru KANNO****** and Masayoshi KOBAYASHI******

(Received April 30, 1986)

Abstract

The dynamic adsorption behavior of O_2, CO and CO_2 on MgO and $MgCO_3$ has been studied in detail at temperatures ranging from 150 to 171°C, by using the transient response method. On $MgCO_3$, no CO adsorbs and no CO oxidation proceeds. CO_2 is reversibly adsorbed obeying the Langmuir isotherm and the heat of adsorption is evaluated to be 2.7 kcal/mol.

On MgO, on the other hand, no CO adsorbs whereas the oxidation of CO easily proceeds and the rate equation is expressed:

$$r = k P_{CO}^{0.63} P_{O_2}^{0.29}$$

The apparent activation energy of reaction is estimated to be 14.6 kcal/mol. CO_2 adsorbs on the surface in both the reversible and irreversible forms. The reversibly adsorbed CO_2 has 4.3 kcal/mol of activation energy for adsorption and 13 kcal/mol for desorption. The irreversibly adsorbed CO_2 can partly desorb by elevating the temperature. A large part of the surface is covered with the strongly adsorbed CO_2, the surface coverage of which is 0.86. Only a small part of the active sites ($\theta = 4.2 \times 10^{-4}$) is available for the adsorption of oxygen and one fifth of the amount is irreversible.

The mode of the transient response curves obtained in the oxidation of CO indicates a typical monotone type suggesting that the reaction rate is controlled by the surface reaction and the desorption of CO_2.

1. Introduction

In our previous papers,[1~9] the oxidation of carbon monoxide has been studied on various metal oxides and metals, especially noting the surface active oxygen species and the kinetic structures, by using the K-I method[1] and the transient response method.[10] CO oxidation easily proceeds on *n*- and *p*-type semiconductors, resulting from the effective activation of surface oxygen and the easy desorption of CO_2 produced. In addition, the number of active sites for oxygen adsorption

* The paper was presented at the Hokkaido regional meeting of the Chemical Society of Japan in the winter period of 1986.

** Chemical Environmental Engineering, Kitami Institute of Technology.
*** Katagiri Store Co.
**** Sanko Control Co.
***** Nippon Softwear Co.
****** Department of Industrial Chemistry, Kitami Institute of Technology.

is relatively larger on the semiconductors than on the insulators. Based on our work, for example, the amounts of the active sites are estimated to be 2.5×10^{15} sites/cm^2 for MnO_2 at -26°C, 4.3×10^{14} sites/cm^2 for Cr_2O_3 at 131- 163°C,[6~8] 9.3×10^{15} sites/cm^2 for Pb_3O_4 at 150°C and 3.2×10^{14} sites/cm^2 for Ag at 20°C, assuming atomic type oxygen to be adsorbed on the active sites. On MnO_2 and Pb_3O_4, it has been speculated that the subsurface oxygen species should be active for the reaction because their active sites are larger than the amount of monolayer.

The turnover frequencies are also estimated to be $1.3\sim6.5\times10^{-5}$ molecules/site•sec at -26°C for MnO_2, $1.0\sim2.8\times10^{-4}$ molecules/site•sec at 163°C for Cr_2O_3, $0.4\sim1.9\times10^{-3}$ molecules/site•sec at 250°C for Pb_3O_4 and $0.5\sim1.6\times10^{-2}$ molecules/site•sec at 20°C for Ag. Generally speaking, the catalytic activity for CO oxidation has been ordered on metal oxides depending on their bulk nature such as *p*-type semiconductors > *n*-type semiconductors > insulators.[11] Extrapoating the Arrhenius plots of the reaction rates for the above tested oxides, the comparison of the turnover frequency at 150°C proposes: Ag (Ag_2O is formed on the surface layer, *p*-type semiconductor, 1.6×10^{-1}sec^{-1}) > MnO_2 (*n*-type semiconductor, 1.2×10^{-3}sec^{-1}) > Cr_2O_3 (*p*-type semiconductor, 1.6×10^{-4}sec^{-1}) > Pb_3O_4 (insulator, 1.6×10^{-5}sec^{-1}). This order does not obey Krylov's rule[10] which illustrates MgO (insulator) to be classified as one of the oxides with very low catalytic activity. This means that the generalized rule can not always apply to specified catalysts which are prepared using different procedures and pretreatments. Our first interest thus is in the actual oxidation activity of MgO compared to other metal oxides.

It seems that CO_2 is absorbed in the magnesium oxide bulk to form $MgCO_3$ which may be catalytically inactive for CO oxidation. The second purpose of this study is to characterize the reactivity of $MgCO_3$-surface against the adsorption of CO and CO_2 and CO oxidation compared to MgO-surface, by using the transient response method.[10]

2. Experimental Method

Catalyst Employed

A commercial magnesium oxide (laboratory grade reagent) from Wako Pure Chemical Company was used for the catalyst and the impurities detected were Cl, 0.01 wt%: PO_4, 0.002 wt%: SO_4, 0.03 wt%: Pb, 0.005 wt%: Zn, 0.02 wt%: As, 0.0005 wt%: Fe, 0.005 wt%. The white fine powder of the sample was dried in an air drying bath at 200°C and pressed at 137 kg/cm^2 for 5 min to make a disk. The pressed disk was ground and sieved so as to become 20~42 mesh(=0.6 mm). The sample was packed in a Pyrex glass tube reactor and dried in a helium stream at 300°C for 24 hr prior to use. The BET surface area was measured by the nitrogen adsorption at -196°C, and found to be 27.5 m^2/g.

Gases Employed

Commercially prepared carbon monoxide (99.9% CO), oxygen (99.9% O_2),

carbon dioxide (99.8% CO_2) and helium (99.99% He) were employed. The purification was carried out by using the reduced Cu to remove O_2 for He and a Molecular Sieve 13X which was cooled at $-78°C$ to remove H_2O from CO and CO_2.

The transient response of the gas components was followed by three gas chromatographs which were prepared at different temperatures and attached by different columns. A Porapak Q column (2 m length, 100~200 mesh) was used for the analysis of CO_2, and a Molecular Sieve 5 A column (1 m length, 40~60 mesh) was used to analyse CO, N_2 and O_2.

Procedure

Fig. 1 illustrates the apparatus used for the concentration jump method. The flow rate of gases was carefully controlled at 160 (±3) ml (NTP)/min by a mass flow controlling valve and the gas was gathered into a mixing chamber. Three gas flow rate controllers, each of which had a different gas composition, were prepared to make a step function of the concentration jump without changing the flow rate. 61.8 g of the catalyst was packed into the reactor (8 mm inner diameter and 120 cm length). The temperature of the reactor was well controlled within an accuracy of ±0.5°C by using a heated fluidized sand bath. The intraparticle gas diffusion effect and the gas film diffusion effect were confirmed to be negligible throughout all the experimental conditions, by testing the catalytic activity for two different catalyst particle sizes, 20~42 (0.6 mm) and 100-200 (0.1 mm) mesh, and for two different flow rates (80 and 160 ml/min) with the same W/F.

The step function of the concentration jump was made by using two four port valves each of which was attached between the three flow controlling systems. The response of the step change between pure He and the mixture of N_2 -He

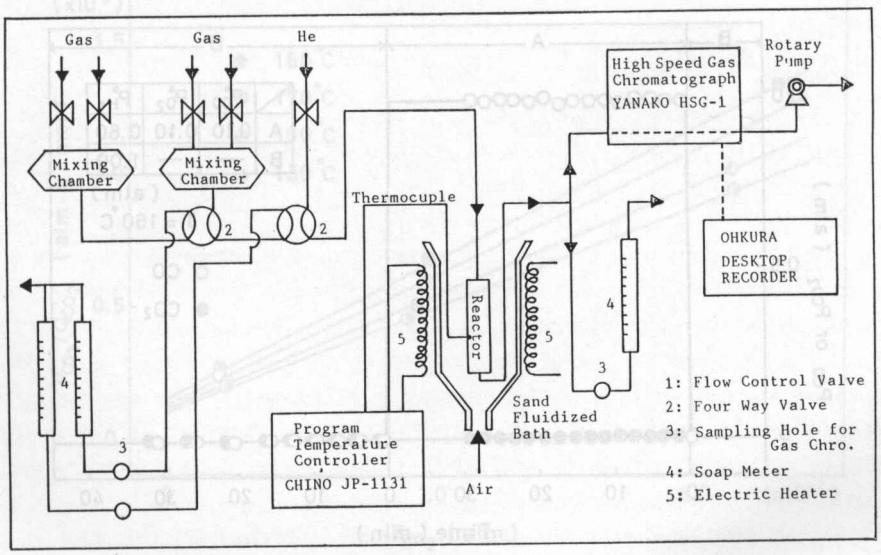

Fig. 1. Experimental aparatus.

(9.6% N_2 and 90.4% He) was completed within fifty seconds, and it was confirmed that the longitudinal gas mixing effect was within ten seconds, suggesting no serious gas mixing effect on the concentration jump function. The measurement of the heat of adsorption for CO_2 was carried out by the GC method dosing one milliliter pulse of CO_2. The flow rate of the carrier gas and the column length of MgO (60~80 mesh) were 30 ml/min and one meter, respectively. Further detailed experimental procedures for the transient response method will be found elsewhere.[10]

3. Experimental Results and Discussion

The following nomenclatures are used for various transient responses: $X-Y$ response designates the response of Y in the outlet stream of the reactor caused by the step change in the inlet concentration of component X, X(inc., 0)-Y response when X is increased from nil and X(dec., 0)-Y when X is decreased into nil.

3-1. Transient Adsorption of CO and CO_2 on $MgCO_3$

Fig. 2 shows the CO(inc., 0)-CO and CO(dec., 0)-CO responses. No delay is observed indicating two possibilities, (1) no or a small amount of CO is adsorbed or (2) CO is irreversibly adsorbed on the surface. The possibility of irreversible adsorption of CO should be rejected, because no desorption of CO was observed even when the catalyst bed was heated in a He stream up to 200°C. One thus may conclude that CO does not adsorb on $MgCO_3$. Fig. 2 also illustrates the CO-CO_2 response. The response clearly shows no formation of CO_2 even though oxygen is present in a gas phase, indicating no catalytic activity of $MgCO_3$ for CO oxidation.

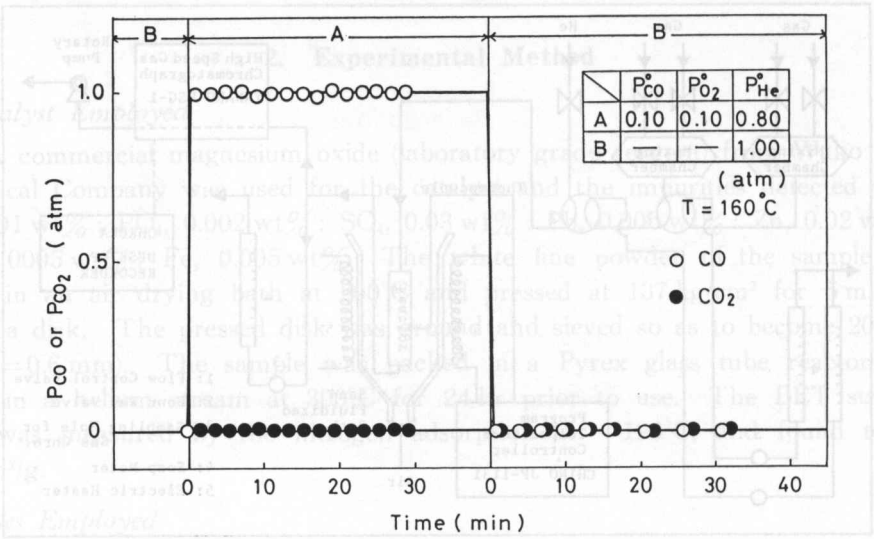

Fig. 2. CO-CO and-CO_2 responses on $MgCO_3$.

Fig. 3 illustrates the CO_2-CO_2 responses on $MgCO_3$ at 160°C. The response clearly shows a delay displaying the adsorption of CO_2. The graphical integrations of the CO_2 (inc., 0)-CO_2 response curve (shaded area, $q_{CO_2}^{ad.}$) and the CO_2 (dec., 0)-CO_2 response curve ($q_{CO_2}^{des.}$) show the adsorbed and desorbed CO_2, respectively. The difference between $q_{CO_2}^{ad.}$ and $q_{CO_2}^{des.}$ corresponds to the amount of the irreversibly adsorbed CO_2. Since $q_{CO_2}^{ad.}$ is in good agreement with $q_{CO_2}^{dec}$, CO_2

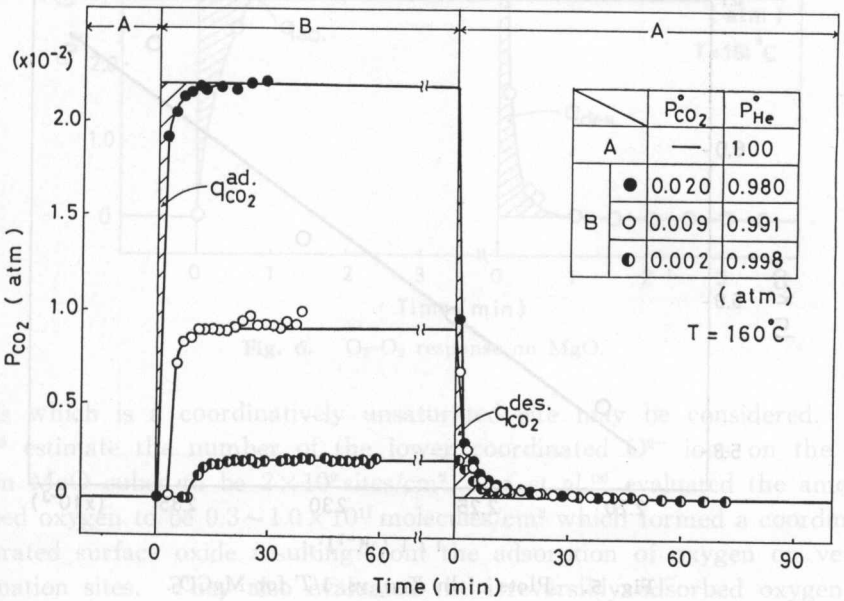

Fig. 3. CO_2-CO_2 responses on $MgCO_3$.

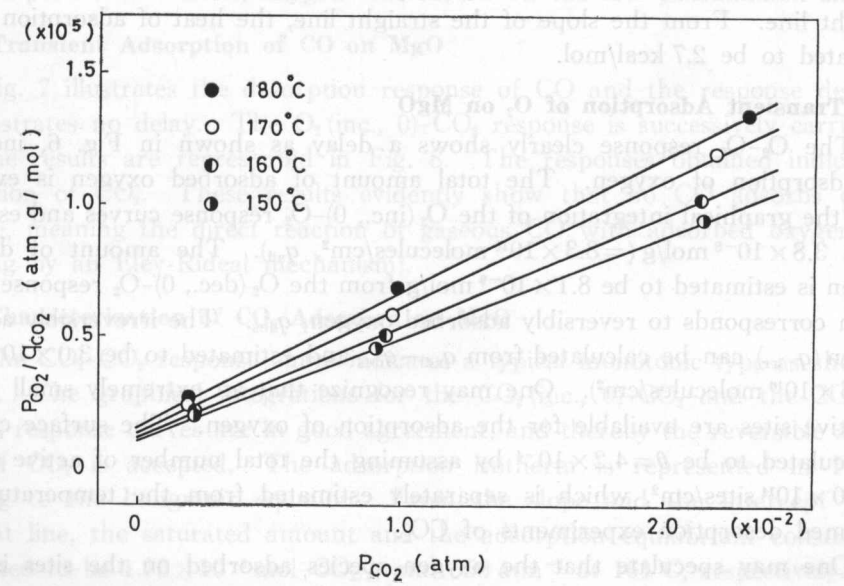

Fig. 4. Adsorption isotherm for CO_2 on $MgCO_3$.

adsorbs in a reversible form. The adsorption isotherms obtained at different temperatures obey the Langmuir isotherm equation and the results are shown in Fig. 4. The saturated amount of adsorbed CO_2 is estimated to be 1.7×10^{-7} mol/g with no dependency on the adsorption temperature, and the equilibrium constants are calculated to be 434 at 150°C 381 at 160°C 362 at 170°C and 340 atm^{-1} at 180°C.

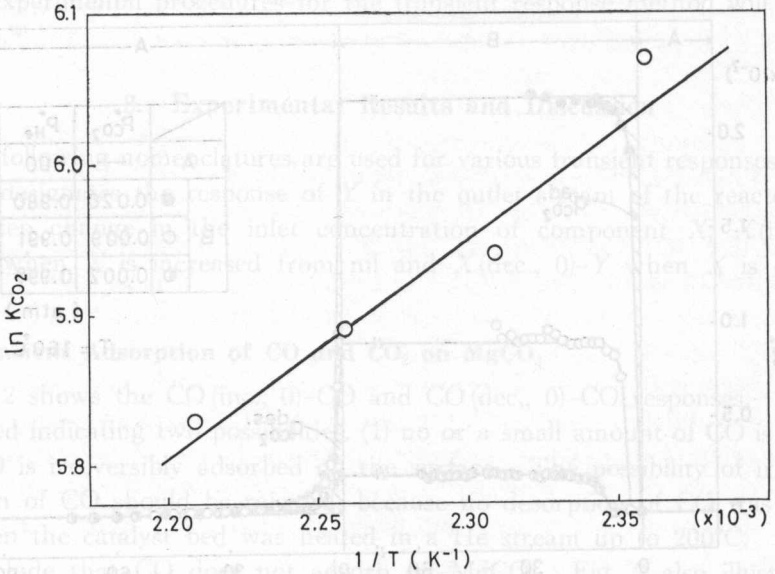

Fig. 5. Plots of ln K_{CO_2} vs. $1/T$ for $MgCO_3$.

Fig. 5 illustrates the plots of ln K_{CO_2} vs. $1/T$, which clearly indicate a good straight line. From the slope of the straight line, the heat of adsorption can be estimated to be 2.7 kcal/mol.

3-2. Transient Adsorption of O_2 on MgO

The O_2-O_2 response clearly shows a delay as shown in Fig. 6, indicating the adsorption of oxygen. The total amount of adsorbed oxygen is evaluated from the graphical integration of the O_2 (inc., 0)-O_2 response curves and estimated to be 3.8×10^{-8} mol/g ($=8.3\times10^{10}$ molecules/cm^2, q_{ad}). The amount of desorbed oxygen is estimated to be 8.1×10^{-9} mol/g from the O_2 (dec., 0)-O_2 response curves, which corresponds to reversibly adsorbed oxygen, q_{des}. The irreversibly adsorbed oxygen (q_{irr}) can be calculated from $q_{ad}-q_{des}$ and estimated to be 3.0×10^{-8} mol/g ($=6.6\times10^{10}$ molecules/cm^2). One may recognize that an extremely small number of active sites are available for the adsorption of oxygen. The surface coverage is calculated to be $\theta=4.2\times10^{-4}$ by assuming the total number of active sites, to be 2.0×10^{14} sites/cm^2, which is separately estimated from the temperature programmed desorption experiments of CO_2.

One may speculate that the oxygen species adsorbed on the sites is active for the oxidation of CO. For the active sites, a corner or an edge of MgO

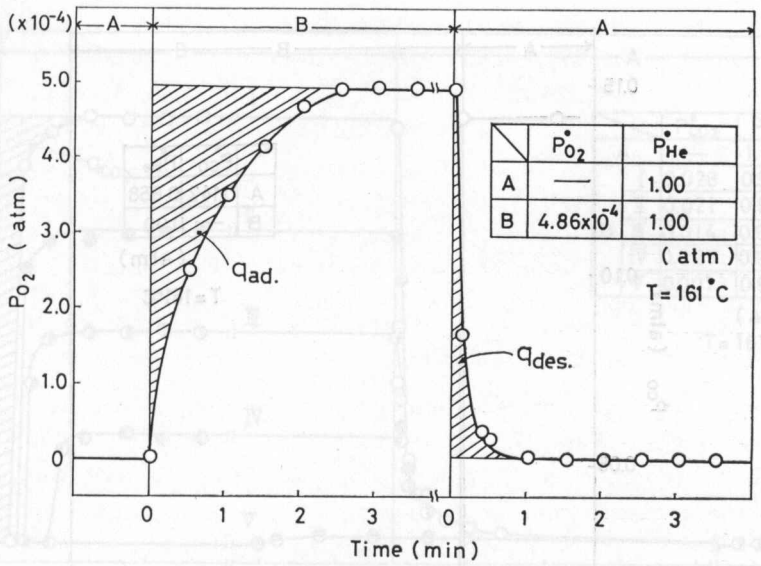

Fig. 6. O_2–O_2 response on MgO.

crystals which is a coordinatively unsaturated site may be considered. Tench et al.[12] estimate the number of the lower coordinated O^{2-} ions on the corner sites on MgO cubes to be 2×10^9 sites/cm^2. Ito et al.[13] evaluated the amount of adsorbed oxygen to be $0.3\sim1.0\times10^{11}$ molecules/cm^2 which formed a coordinatively unsaturated surface oxide resulting from the adsorption of oxygen on very low coordination sites. They also evaluated the irreversibly adsorbed oxygen to be around 6.0×10^{10} molecules/cm^2, which was very close to our result. Based on these experimental results, oxygen will adsorb on the low coordination sites.

3-3. Transient Adsorption of CO on MgO

Fig. 7 illustrates the desorption response of CO and the response definitely demonstrates no delay. The O_2 (inc., 0)–CO_2 response is successively carried out and the results are represented in Fig. 8. The responses obtained indicate no formation of CO_2. These results evidently show that no CO adsorbs on the surface, meaning the direct reaction of gaseous CO with adsorbed oxygen (progressing by an Eley-Rideal mechanism).

3-4. Characterization of CO_2 Adsorbed on MgO

The CO_2–CO_2 response curve indicates a typical monotonic type as shown in Fig. 9. The graphical integrations for the CO_2 (inc., 0)–CO_2 and the CO_2 (dec., 0)–CO_2 response curves are in good agreement, and thereby the reversible adsorption of CO_2 is accepted. The adsorption isotherm is represented in Fig. 10 relating to the Langmuir equation. From the slope and the intercept of the straight line, the saturated amount and the adsorption equilibrium constant are estimated to be 1.75×10^{-5} mol-CO_2/g and 550 atm^{-1} at 161°C, respectively. The saturated amount of adsorbed CO_2 is independent of the adsorption temperature.

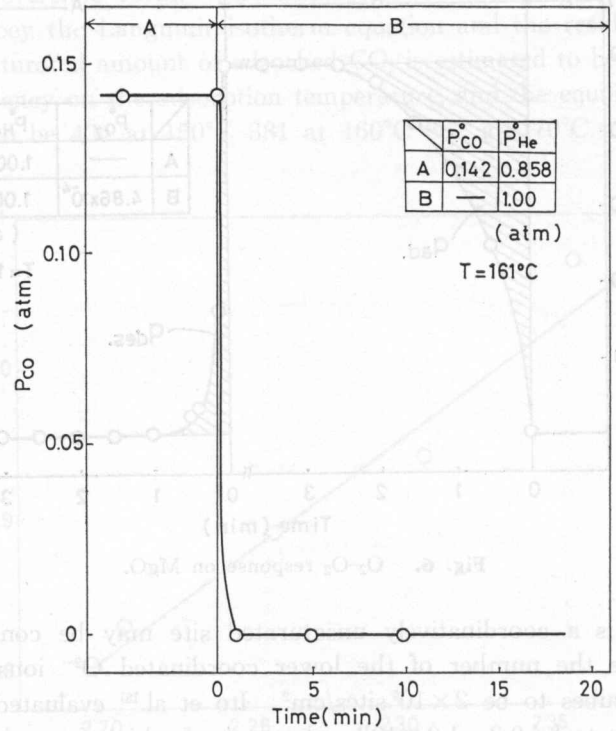

Fig. 7. CO(dec., 0)–CO response on MgO.

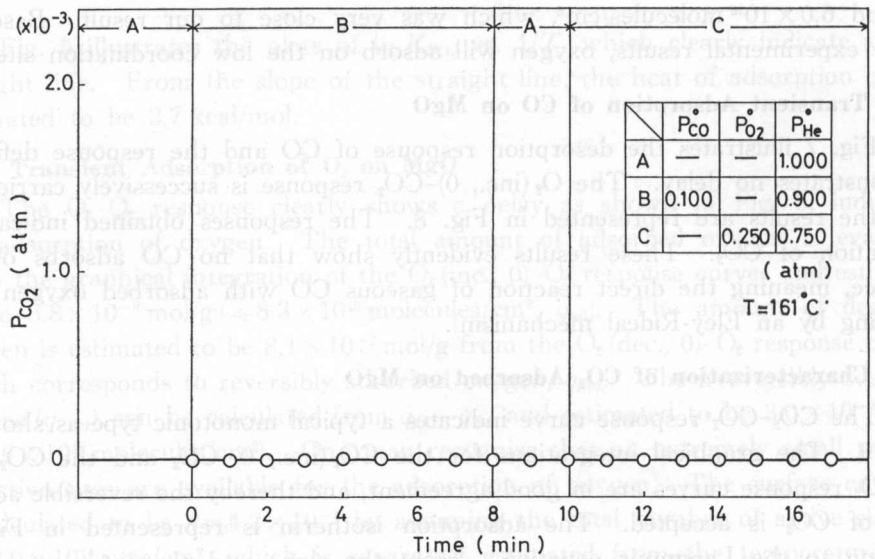

Fig. 8. CO–CO_2 and O_2–CO_2 responses on MgO.

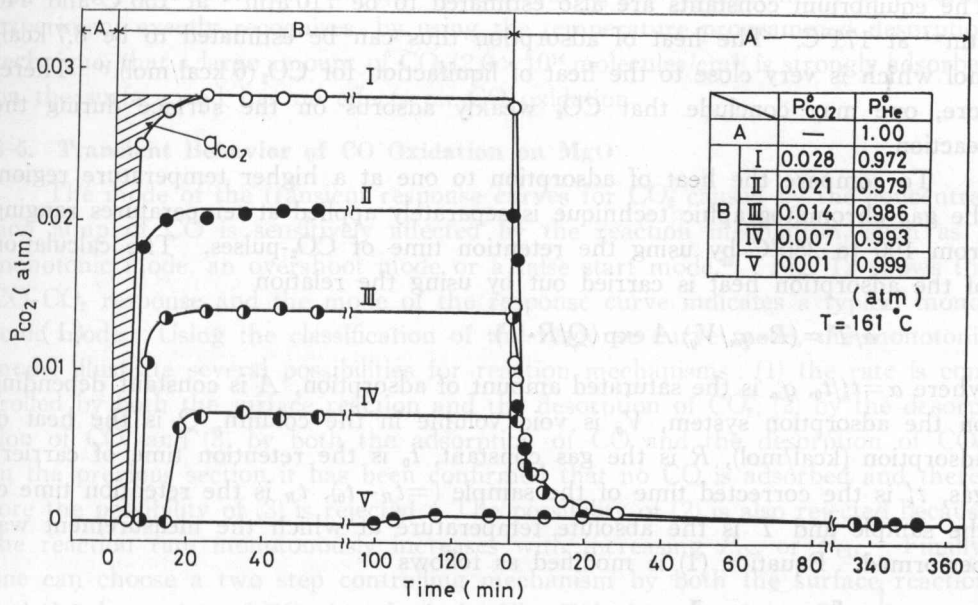

Fig. 9. CO_2–CO_2 responses on MgO.

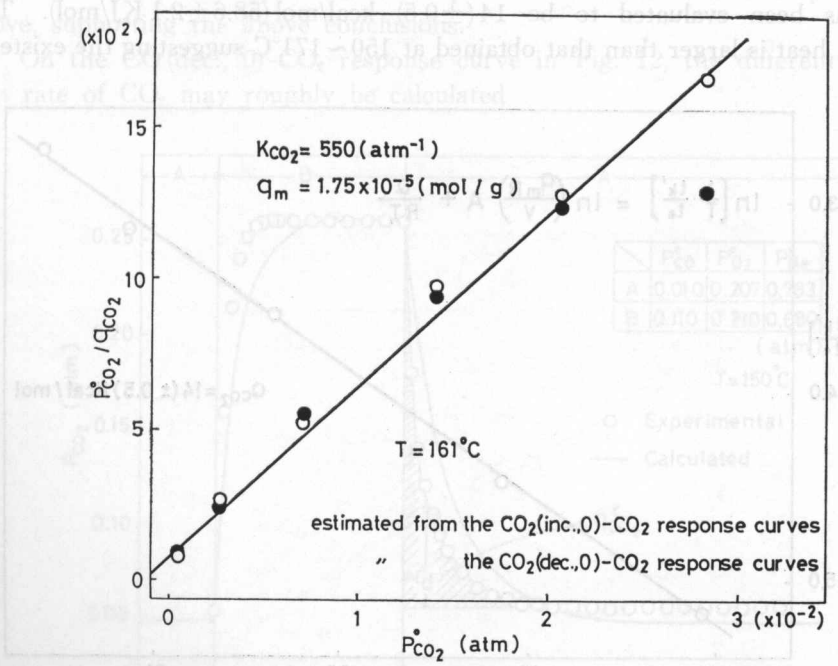

Fig. 10. Langmuir plots of adsorbed CO_2 on MgO.

The equilibrium constants are also estimated to be 710 atm^{-1} at 150°C and 440 atm^{-1} at 171°C. The heat of adsorption thus can be estimated to be 8.7 kcal/mol which is very close to the heat of liquifaction for CO_2 (6 kcal/mol).[14] Therefore, one may conclude that CO_2 weakly adsorbs on the surface during the reaction.

To compare the heat of adsorption to one at a higher temperature region, the gas chromatographic technique is separately applied at temperatures ranging from 190 to 280°C by using the retention time of CO_2-pulses. The calculation of the adsorption heat is carried out by using the relation

$$\alpha/T = (R \cdot q_m/V_g)\, A \exp(Q/R \cdot T) \qquad (1)$$

where $\alpha = t_k'/t_0$, q_m is the saturated amount of adsorption, A is constant depending on the adsorption system, V_g is void volume in the column, Q is the heat of adsorption (kcal/mol), R is the gas constant, t_0 is the retention time of carrier gas, t_k' is the corrected time of the sample ($=t_R - t_0$), t_R is the retention time of the sample and T is the absolute temperature at which the measurement was performed. Equation (1) is modified as follows

$$\ln\left[(1/T)\,(t_k'/t_0)\right] = C + Q/R \cdot T \qquad (2)$$

where $C = \ln(R \cdot q_m/V_g)A$

Fig. 11 illustrates the estimation of the heat of adsorption by the GC method and it has been evaluated to be 14 (±0.5) kcal/mol (58.6±2.1 KJ/mol). This adsorption heat is larger than that obtained at 150～171°C suggesting the existence

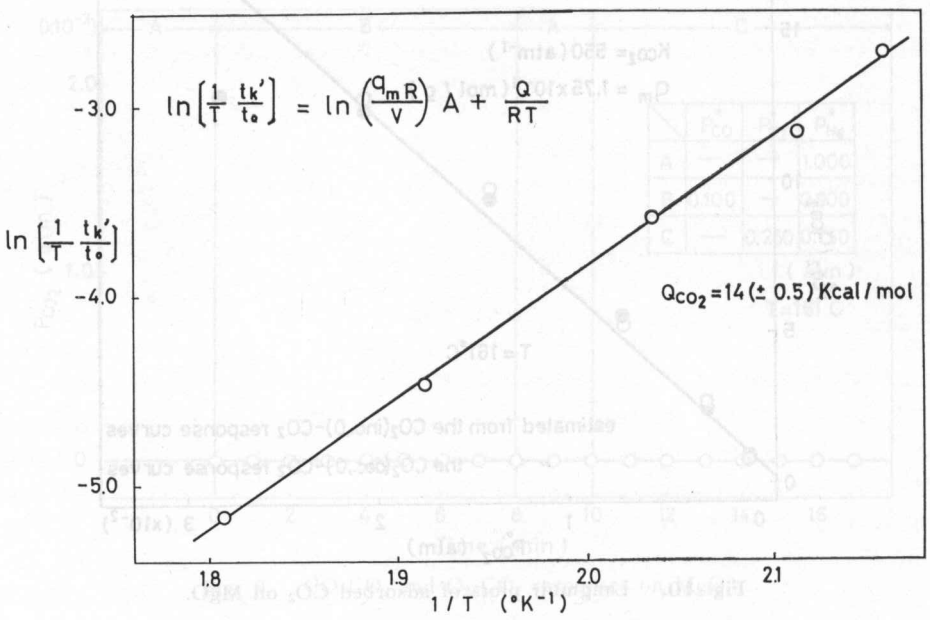

Fig. 11. Estimation of the heat of adsorption for CO_2 on MgO by the Pulse technique.

of strongly adsorbed CO_2 on the surface during CO oxidation. The separate experiment exactly recognizes, by using the temperature programmed desorption technique, that a large amount of CO_2 (2.0×10^{14} molecules/cm^2) is strongly adsorbed on the surface and has no effects on CO oxidation.

3-5. Transient Behavior of CO Oxidation on MgO

The mode of the transient response curves for CO_2 caused by the concentration jump of CO is sensitively affected by the reaction mechanism, such as a monotonic mode, an overshoot mode or a false start mode.[15] Fig. 12 shows the CO-CO_2 response and the mode of the response curve indicates a typical monotonic mode. Using the classification of the response curve mode, the monotonic model illustrate several possibilities for reaction mechanisms: (1) the rate is controlled by both the surface reaction and the desorption of CO_2, (2) by the desorption of CO_2 and (3) by both the adsorption of CO and the desorption of CO_2. In the previous section it has been confirmed that no CO is adsorbed and therefore the possibility of (3) is rejected. The possibility of (2) is also rejected because the reaction rate monotonously increases with increasing P_{CO} or P_{CO_2}. Finally, one can choose a two step controlling mechanism by both the surface reaction and the desorption of CO_2, based on the Eley-Rideal mechanism. The computer simulation technique is separately applied to distinguish the rival kinetic models and to determine the kinetic parameters. The best fitting kinetic parameters estimated clearly show the slower steps to be the same two steps presented above, supporting the above conclusions.

On the CO (dec., 0)-CO_2 response curve in Fig. 12, the differential desorption rate of CO_2 may roughly be calculated

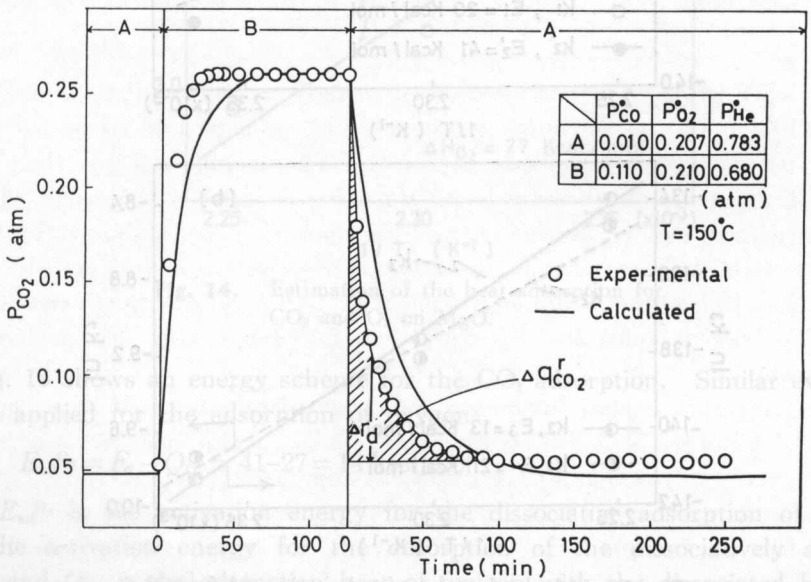

Fig. 12. CO-CO_2 response on MgO.

$$\Delta r_d = k_d \Delta\theta_{CO_2} \quad (3)$$

where Δr_d is the desorption rate of CO_2 (mol/g·min), $\Delta\theta_{CO_2} = \Delta q_{CO_2}/q_m(-)$, k_d is the apparent desorption rate constant of CO_2 (mol/g·min), q_{CO_2} is the differential amount of adsorbed CO_2 at any elapsed time which is displayed by a shaded area in the CO (dec., 0)-CO_2 response curve (mol/g) and q_m is the saturated amount of adsorbed CO_2 ($=1.75\times10^{-5}$ mol/g). r_d is easily calculated from the height of the CO (dec., 0)-CO_2 response curve as shown in Fig. 12, by using the following equation,

$$\Delta r_d = \Delta x/\Delta(W/F) = 1.08\times10^{-4}\Delta P_{CO_2} \quad (4)$$

where Δx, W, F and ΔP_{CO_2} are conversion of CO, catalyst weight (61.8 g), molar flow rate of CO (mol/min) and the height of P_{CO_2} at the CO (dec., 0)-CO_2 response curve, respectively. The plots of Δr_d vs. θ_{CO_2} represent a good straight line and k_d is evaluated from the slope of the line as 8.8×10^{-7} mol/g min. The obtained k_d is close to $k_3 = 7.37\times10^{-7}$ mol/g min which is estimated by the computer simulation technique. From this agreement, one may see that the graphical analysis of the desorption curves has no serious error for estimating the desorption rate

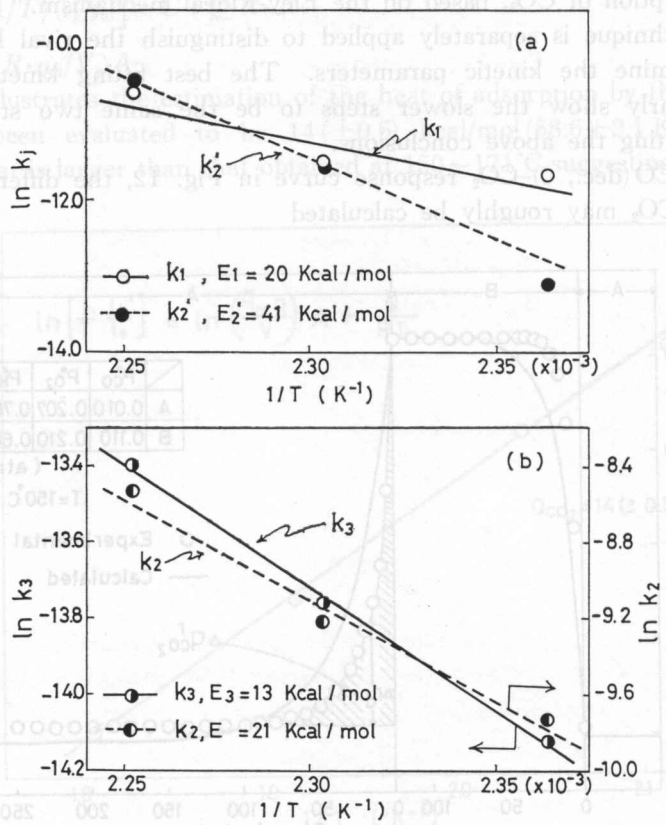

Fig. 13. Arrhenius plots for k_j estimated from the computer simulation technique, on MgO.

constant.

The values of k_j estimated by the computer simulation technique are presented in Fig. 13. Here, k_1 is the rate constant for the surface reaction $CO+O\cdot S$, k_2 and k_2' are for the equilibrium reaction $O_2 \rightleftarrows 2O\cdot S$, and k_3 is for $CO_2\cdot S \rightarrow CO_2(g)$. Arrhenius plots for k_j display good straight lines. The plots of equilibrium constants K_j indicate a similar tendency as shown in Fig. 14. The activation energy of CO_2 desorption and the adsorption heat of CO_2 are evaluated to be $E_3=13$ kcal/mol and $Q_{CO_2}=8.7$ kcal/mol, respectively. The activation energy of CO_2 adsorption thereby can be estimated

$$E_{ad}^{CO_2} = E_3 - Q_{CO_2} = 13-8.7 = 4.3 \text{ kcal/mol} \qquad (5)$$

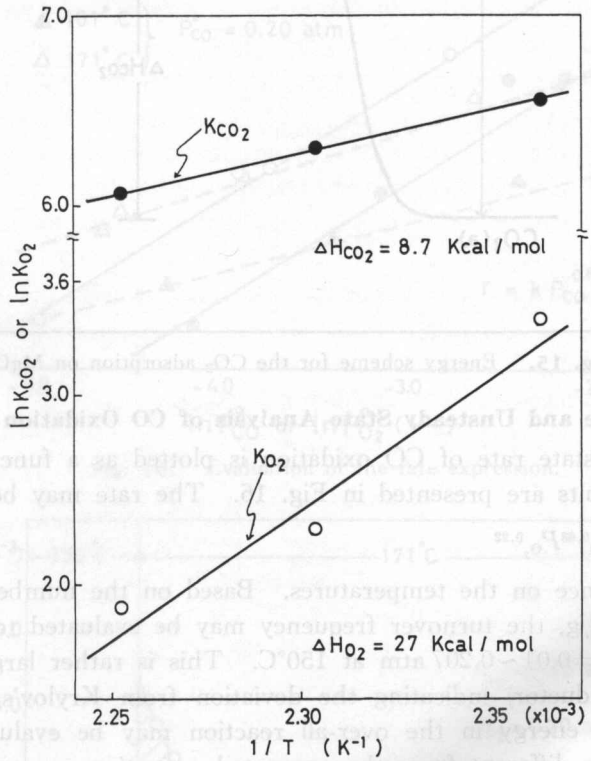

Fig. 14. Estimation of the heat adsorption for CO_2 and O_2 on MgO.

Fig. 15 shows an energy scheme for the CO_2 adsorption. Similar evaluation may be applied for the adsorption of oxygen

$$E_{ad}^{O_2} = E_2 - Q_{O_2} = 41-27 = 14 \text{ kcal/mol} \qquad (6)$$

where $E_{ad}^{O_2}$ is the activation energy for the dissociative adsorption of oxygen, E_2 is the activation energy for the desorption of the dissociatively adsorbed oxygen and Q_{O_2} is the adsorption heat of oxygen with the dissociated form.

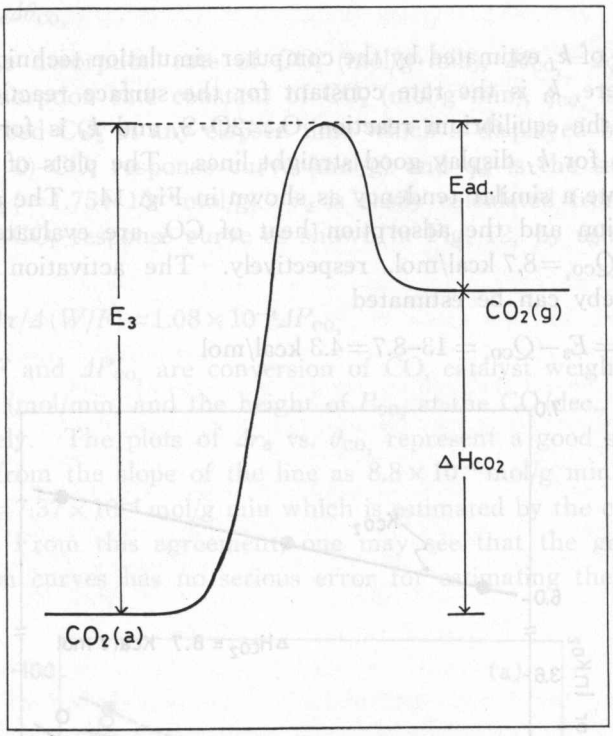

Fig. 15. Energy scheme for the CO_2 adsorption on MgO.

3-6. Steady State and Unsteady State Analysis of CO Oxidation

The steady state rate of CO oxidation is plotted as a function of P_{CO} and P_{O_2}, and the results are presented in Fig. 16. The rate may be expressed

$$r = kP_{CO}^{0.63}P_{O_2}^{0.22} \qquad (7)$$

with no dependence on the temperatures. Based on the number of active sites of 1.75×10^{-5} mol/g, the turnover frequency may be evaluated to be $5.3\times10^{-5}\sim 3.1\times10^{-4}$ at $P_{CO}=0.01\sim0.207$ atm at 150°C. This is rather larger than that of Cr_2O_3 (P-semiconductor) indicating the deviation from Krylov's rule. The apparent activation energy in the over-all reaction may be evaluated to be 14.6 kcal/mol which is different from the computed activation energy for the surface reaction ($E_i=20$ kcal/mol, estimated from Fig. 13 (a)). This disagreement means that the reaction is controlled by more than two elementary steps including the surface reaction.

The temperature jump technique can conveniently be used to evaluate the irreversibly adsorbed CO_2. The experiment was carried out between 150 and 171°C. After the reaction steady state was completed at $P_{CO}^{\circ}=0.21$, $P_{O_2}^{\circ}=0.20$, $P_{He}^{\circ}=0.59$ atm and at 150°C, the temperature was jumped up to 171°C in a stepwise fashion and the response of CO_2 at the outlet stream was followed. The response curve of CO_2 obtained was considerably greater than the expected curve which was calculated from the computer simulation procedure, indicating

a typical over-shoot mode. This difference between the experimental and calculated transient curves can easily be estimated as a function of time as shown in Fig. 17. From the curve, one may recognize the reaction steady state to be completed within 18 min and the curve shows an instanstaneous maximum and then a monotonic decrease. Here, when the readsorption of CO_2 formed is negligibly small, the desorption rate of CO_2 can be calculated from the following equation,

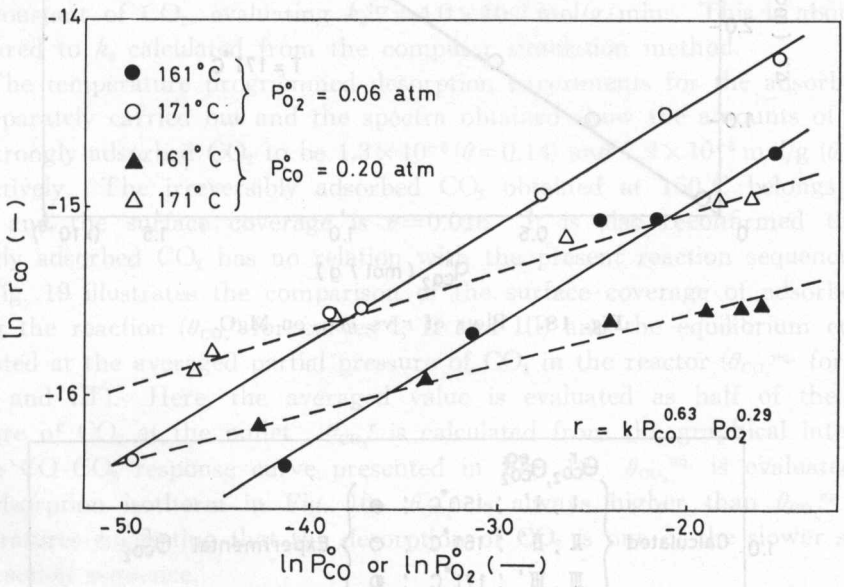

Fig. 16. Evaluation of the rate expression.

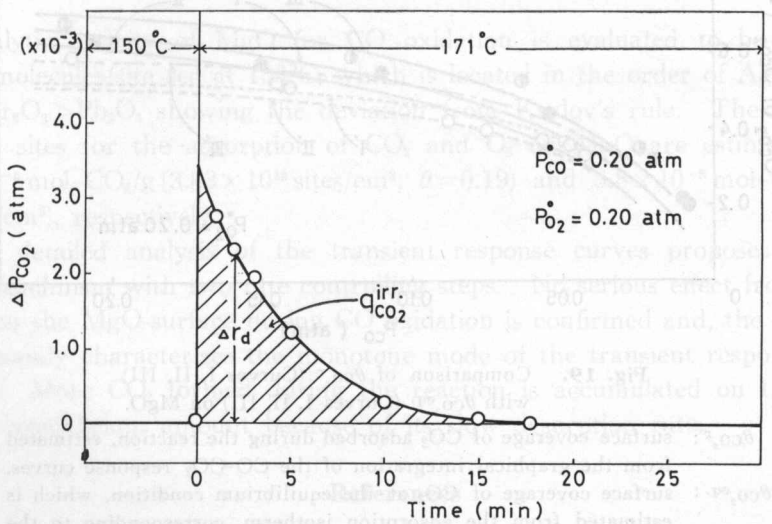

Fig. 17. T (inc., 150°C)-CO_2 response on MgO.

P_{CO_2}: difference between the calculated and experimental response curves.
$q^{irr}_{CO_2}$: the amount of CO_2 which is irreversibly adsorbed at 150°C.

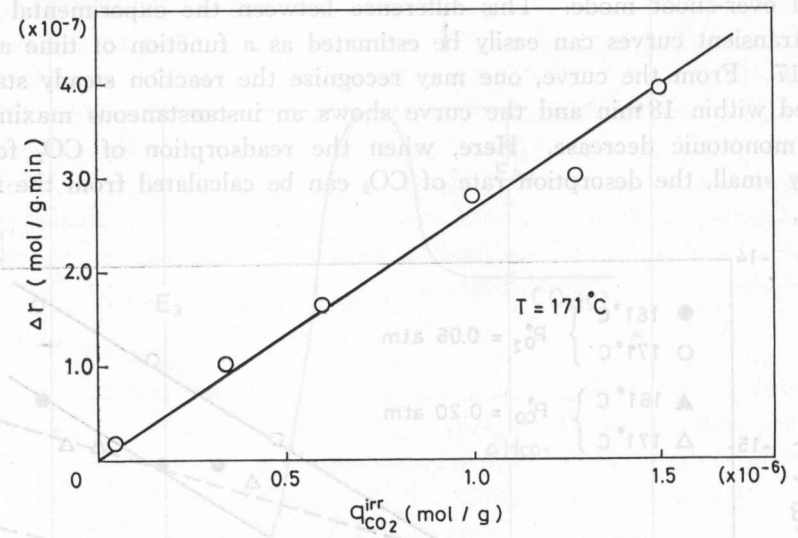

Fig. 18. Plots of r vs. q_{CO_2} on MgO.

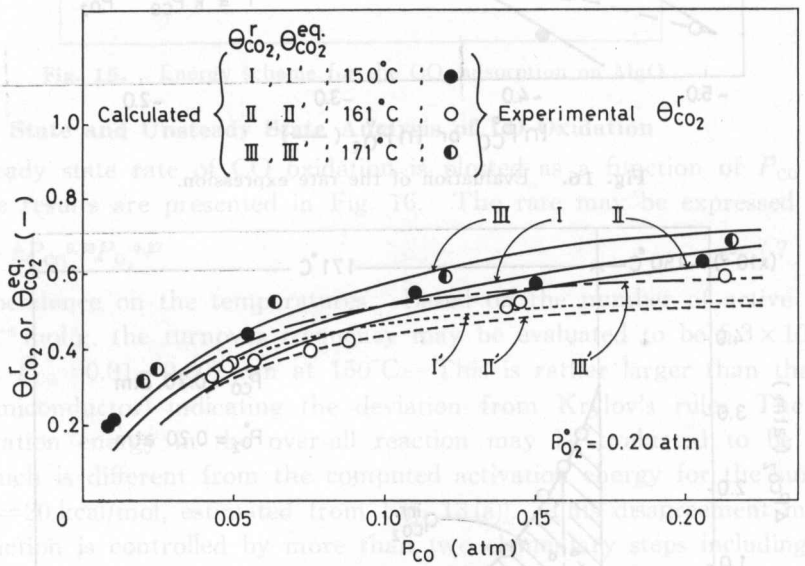

Fig. 19. Comparison of $\theta_{CO_2}{}^{r}$ (Curves I, II, III) with $\theta_{CO_2}{}^{eq.}$ (Curves I, II, III) on MgO.

$\theta_{CO_2}{}^{r}$: surface coverage of CO_2 adsorbed during the reaction, estimated from the graphical integration of the CO–CO_2 response curves.

$\theta_{CO_2}{}^{eq.}$: surface coverage of CO_2 at the equilibrium condition, which is estimated from the adsorption isotherm, corresponding to the avaraged concentration of CO_2 formed in the reactor.

$$r_d^{irr} = k_d^{irr}\theta_{CO_2}^{irr} \quad (8)$$

where r_d^{irr} is the differential desorption rate of strongly adsorbed CO_2 (mol/g·min), k_d^{irr} is the apparent desorption rate constant (mol/g·min), $\theta_{CO_2}^{irr}$ is the surface coverage of CO_2 (corresponds to $q_{CO_2}^{irr}/q_{CO_2}^{max}$), $q_{CO_2}^{irr}$ is the amount of strongly adsorbed CO_2 at 150°C and $q_{CO_2}^{max}$ is the total amount of CO_2 desorbed at 171 °C ($1.5(\pm 0.1)\times 10^{-6}$ mol/g). The plot of r_{CO_2} vs. $q_{CO_2}^{irr}$ gives a good straight line as shown in Fig. 18. The slope of the line proposes the apparent desorption rate constant of CO_2, evaluating $k_d^{irr}=4.0\times 10^{-7}$ mol/g·min. This is about 54% compared to k_3 calculated from the computer simulation method.

The temperature programmed desorption experiments for the adsorbed CO_2 are separately carried out and the spectra obtained show the amounts of weakly and strongly adsorbed CO_2 to be 1.3×10^{-5} ($\theta=0.14$) and 7.9×10^{-5} mol/g ($\theta=0.86$), respectively. The irreversibly adsorbed CO_2 obtained at 150°C belongs to the latter and the surface coverage is $\theta=0.016$. It is also reconfirmed that the strongly adsorbed CO_2 has no relation with the present reaction sequence.

Fig. 19 illustrates the comparison of the surface coverage of adsorbed CO_2 during the reaction ($\theta_{CO_2}^{r}$ for curves I, II and III) and the equilibrium coverage estimated at the averaged partial pressure of CO_2 in the reactor ($\theta_{CO_2}^{eq.}$ for curves I′, II′ and III′). Here, the averaged value is evaluated as half of the partial pressure of CO_2 at the outlet. $\theta_{CO_2}^{r}$ is calculated from the graphical integration of the CO-CO_2 response curve presented in Fig. 12. $\theta_{CO_2}^{eq.}$ is evaluated from the adsorption isotherm in Fig. 10. $\theta_{CO_2}^{r}$ is always higher than $\theta_{CO_2}^{eq.}$ at all temperatures suggesting that the desorption of CO_2 is one of the slower steps in the reaction sequence.

4. Conclusions

Catalytic activity of MgO for CO oxidation is evaluated to be $5\times 10^{-5}\sim 3\times 10^{-4}$ molecules/site sec at 150°C, which is located in the order of $Ag > MnO_2 > MgO > Cr_2O_3 > Pb_3O_4$ showing the deviation from Krylov's rule. The population of active sites for the adsorption of CO_2 and O_2 on MgO are estimated to be 1.75×10^{-5} mol-CO_2/g (3.83×10^{13} sites/cm^2, $\theta=0.19$) and 3.8×10^{-8} mol-O_2/g (8.3×10^{10} sites/cm^2), respectively.

The detailed analysis of the transient response curves proposes an Eley-Rideal meachnism with two rate controlling steps. No serious effect from $MgCO_3$ formed on the MgO-surface during CO oxidation is confirmed and, the desorption of CO_2 mainly characterizes the monotone mode of the transient response curves obtained. More CO_2 formed during the reaction is accumulated on the surface than the equilibrium amount because of its slow desorption rate.

References

1) Kobayashi, M., Matsumoto, H. and Kobayashi, H. J. Catal., **21**, 48 (1971).
2) Kobayashi, M. and Kobayashi, H. J. Catal., **27**, 150 (1972).
3) Kobayashi, M. and Kobayashi, H. J. Catal., **27**, 108 (1972).

4) Kobayashi, M. and Kobayashi, H. J. Catal. **27**, 114 (1972).
5) Kobayashi, M. and Kobayashi, H. J. Catal., **36**, 74 (1975).
6) Kobayashi, M. and Kobayashi, H. Bull, Chem. Soc. Jap., **49**, 3009 (1976).
7) Kobayashi, M., Date, T. and Kobayashi, H. Bull. Chem. Soc. Jap., **49**, 3014 (1976).
8) Kobayashi, M. and Kobayashi, H. Bull. Chem. Soc. Jap., **49**, 3018 (1976).
9) Kobayashi, M. and Kobayashi, H. J. Chem. Soc. Faraday Trans. 1. **80**, 1221 (1984).
10) Kobayashi, H. and Kobayashi, M. Catal. Rev. Eng. Sci., **10**, 139 (1975).
11) Krylov, O. B. Kinet. Katal., **3**, 502 (1962).
12) Coluccia, S., Barton, A. and Tench, A. J. J. Chem. Soc., Faraday Trans. 1, **77**, 2203 (1981).
13) Ito, T., Sekino, T., Moriai, N. and Tokuda, T. J. Chem. Soc., Faraday Trans., 1., **77**, 2181 (1981).
14) Trapnell, B. M. "Chemisorption", Butterworths Scientific Publication (1955).